POLITECNICO
MILANO 1863

SCUOLA DI INGEGNERIA INDUSTRIALE
E DELL'INFORMAZIONE

EXECUTIVE SUMMARY OF THE THESIS

3D Printable polymer-leather composites for industrial waste recovery and circular economy

Master's thesis in Materials Engineering and Nanotechnology – Ingegneria dei Materiale e delle Nanotecnologie

AUTHOR: DAVIDE NEGRI

ADVISOR: MARINELLA LEVI

ACADEMIC YEAR: 2022-2023

1 Introduction

Leather, a refined byproduct of animal hides and skins, exemplifies circularity by originating from waste in the food chain. Despite the prevalence of modern materials like plastics and synthetics, leather endures due to its superior quality and aesthetic appeal. Leather and related products rank among the most globally traded commodities. As of 2022, the global leather products market reached a size of USD 440.64 billion, with Europe contributing USD 166.22 billion. Future projections anticipate the leather market's growth, reaching $738.61 billion in 2030 from an estimated $468.49 billion in 2023. [1] If from the economic side these numbers are encouraging for the sector, from the environmental side it is the opposite. Leather industry consumes 1 Mg of raw materials and 15,000 to 120,000 m3 of water to produce just 0.25 Mg of leather. This process yields 15–50 Mg of wastewater, 400–700 kg of solid waste, and emissions of odors, greenhouse gases (CO_2, H_2S, NH_3), and volatile organic compounds. The magnitude of these environmental effects depends on the technology and treatment methods employed in tanneries. [2] This is where 3D printing (3DP) comes to our rescue, with the idea of recycling leather waste, which takes on the function of a polymer matrix filler, for the creation of fashion objects, to reduce the production of leather products. 3DP is a fabrication process in which three-dimensional parts are produced through layer-wise sequential deposition of material, from 3D model data. It offers some advantages as design flexibility, cost of geometric complexity, dimensional accuracy, time and cost efficiency in production run. It presents also aims, that need to be investigated, such as multi-material parts, surface finishing, anisotropy, build speed. Direct Ink Writing (DIW) is the 3DP technique adopted in this work. It is a material extrusion method where liquid ink, housed in a cartridge, is extruded through a nozzle and, upon external stimuli like UV light or temperature, the ink crosslinks into a solid material. It's a versatile 3DP method with potential for various materials, multi-material printing, and cost-effectiveness. Challenges persist in adapting complex functional or composite inks. DIW employs pneumatic, mechanical piston, or screw extrusion for material

deposition, controlled by air pressure, piston motion, or screw rotation, respectively. The first mechanism is the one used in the project. [3] By employing Life Cycle Assessment (LCA), an extensive approach to assess the environmental effects of products from inception to disposal, a comparison was conducted between the environmental impacts of leather production and 3DP utilizing leather waste. LCA considers emissions and resource depletion. Important standards and frameworks for LCA encompass ISO 14040 and 14044, as well as resources such as the International Reference Life Cycle Data System (ILCD) Handbook. [4]

2 Materials and methods

2.1 Materials

Milled leather remnants were sourced from Stazione Sperimentale Italiana Pelli (SSIP), Italy. The material comprises shaved glutaraldehyde-tanned leather, pre-sieved through a 0.5 mm sieve. The ethoxylate bisphenol A diacrylate resin, denoted as SR349, was procured from Arkema, distributed locally by Came S.r.l., Italy. Ethyl phenyl (2, 4, 6-trimethyl benzoyl) phosphinate, designated TPO-L, was acquired from Lambson Limited, UK. Silica, dicumyl peroxide, triethoxy(octyl)silane, poly(vinyl alcohol) or PVA, and glycerol were obtained from Sigma-Aldrich, locally distributed by Merk Life Science S.r.l., Italy. Additionally, 2-Hydroxy-4′-(2-hydroxyethoxy)-2-methylpropiophenone, known as Irgacure 2959, was sourced from BASF, Germany.

Rigid and flexible matrix are investigated, respectively SR349 and PVA. Each matrix was first formulated with silica to understand mechanical properties, then moved on to the formulation of interest with leather.

SR349 resin, combined with varying silica concentrations (5%, 10%, 15%, 20% w/w), underwent thorough investigation. Initially, silica was dispersed in acetone through ultrasonic processing at room temperature for 45 minutes. The resultant solution was then added to SR349 along with 3% w/w TPO-L, and the mixture was stirred at 100°C until acetone evaporation. Leather incorporation at 10%, 15%, and 20% w/w ratios involved dispersing a gram of leather in 50 ml ethanol with 6% w/w silane, stirring at 50°C for 26 hours, rinsing thrice, and evaporating ethanol at 100°C. Latter formulations received dicumyl peroxide (0.3% w/w) for a dual curing approach, assuming the leather shields UVs.

PVA was initially assessed with silica by dispersing different silica percentages (10%, 15%, 20% w/w with respect to water) in distilled water using an ultrasonic processor. After 45 minutes at room temperature, PVA and photoinitiator Irgacure 2959 (3% w/w with respect to water) were added. In the leather-infused formulation, the same resin formulation was used, with the filler added at the end (20%, 25%, 30% w/w with respect to the matrix) along with 0.3% w/w dicumyl in distilled water and 20% w/w glycerol at room temperature.

2.2 Methods

2.2.1 Life Cycle Assessment (LCA)

A comparative LCA has been carried out, comparing virgin leather and recycled leather + resin material. As regard the matrix, acrylic resin has been considered in this case. The Life Cycle Impact Assessment method used is ReCiPe Midpoint+ (H) and the categories analysed are Climate Change (kg CO_2 eq) and Acidification (kg SO_2 eq). in each category production, distribution, and disposal step are taken into account. The LCA analysis is based on literature documents [5], [6]. Environmental impacts (EI), for both parameters, of composite material were calculated for each composition using the following formula, Eq. 1:

$$\begin{aligned} EI &= EI_{Recycled\ leather\ from\ waste} \cdot x \\ &+ EI_{Recycled\ leath\quad from\ hides} \cdot x \\ &+ EI_{Acrylic\ resin} \cdot (1\text{-}x) \end{aligned} \qquad 1$$

where EI are respectively the environmental impact of 1 kg of acrylic resin and recycled leather; x represents the percentages of leather.

2.2.2 3D printer

A low-cost, home-assembled Chimera printer with a pneumatic extruder and 12 LEDs facilitated UV-3D printing of composite mixtures. For leather samples, a dual curing process was employed, involving UV curing after each printed layer under LED lamps for initial stabilization. After completion, a second UV curing step with a UVA lamp and a thermal curing process in an oven ensured complete curing.

2.2.3 Filler dimensional characterization

Filler dimensional characterization utilized optical microscopy, assessing leather particle dimensions and shape parameters analyzing the ratio between filler area and circle area drawn to inscribe the filler. The diameter (d) of the latter was defined as the characteristic dimension of the leather. Eq. 2 shows the parameter.

$$P = \frac{A_{filler}}{A_{circle}} \qquad 2$$

2.2.4 Rheological tests

Rheological tests involved frequency and amplitude sweeps, as well as a thixotropy test, essential for extrusion and filament behavior. High shear rates prompted sample displacement, necessitating the assessment of complex viscosity through the first test. The amplitude sweep test explored increasing shear amplitudes, determining the crosspoint between storage (G') and loss (G'') moduli, crucial for identifying the yield stress and yield strain—essential parameters for DIW. A final test simulated printing conditions through oscillatory steps, mimicking cartridge, extrusion, and platter phases. Notably, the ability of G' to surpass G'' in the third period indicated material cessation immediately post-extrusion, a desirable trait for effective printing.

2.2.5 Printability tests

Printability tests included filament uniformity, fusion, and pore geometry assessment, crucial for evaluating shape fidelity. The first one investigates the uniformity and shape fidelity of extruded filament with the Eq. 3, where d_i and d_{av} are respectively the measured and average diameter.

$$U = \frac{\sum_{i=1}^{N} |d_i - d_{av}|}{N} \qquad 3$$

The second test assessed the fusion of adjacent filaments. Lower yield stress led to longer fused segments, impacting resolution. Parameters included filament distances f_d, fused segment length f_s, and filament thickness f_t. The evaluation parameter, the ratio of fused filament length to thickness, indicated printability and stability post-extrusion. A ratio closer to 1, with increased distances, signified enhanced printability.

The final test assesses the geometrical accuracy of cross filaments using the Eq. 4 of printability index Pr, determined by the area and perimeter of pores with an ideal 0-90° laydown pattern. Deviations from the ideal value of 1 indicate irregular shapes—higher values suggest discontinuity and nonlinear print direction, while lower values indicate rounder pore shapes, potentially linked to nonoptimal gelation or low material viscosity affecting post-extrusion stability.

$$P_r = \frac{l^2}{16A} \qquad 4$$

2.2.6 Gel content

Gel content, indicating crosslinking, was assessed post-curing through solvent extraction. Eq. 5 is used for the test:

$$Gel\% = \left(1 - \frac{w_0 - w_f}{w_0}\right) \times 100 \qquad 5$$

where w_0 and w_f are respectively starting and final mass after the drying. In PVA cases, w_0 takes into account lost glycerol, due to its dissolution in water.

2.2.7 Ultraviolet light-DSC (UV-DSC)

UV-DSC gauged functional group reactivity to UV light and measured the curing percentage with Eq. 6.

$$1 - \frac{\frac{H_{PC}}{\frac{1}{1+X}}}{\frac{H}{\frac{1}{1+X}}} \qquad 6$$

H and H_{PC} are respectively the enthalpy of the sample pre and post curing; 1 in the denominator is the resin quantity; X represents the filler fraction (in PVA cases 0.8 has to add to indicates the glycerol fraction).

2.2.8 Differential Scanning Calorimetry (DSC)

DSC determined material glass transition temperature and heating curing percentage. Formulas are the same as above.

2.2.9 Uniaxial tensile test

Uniaxial tensile testing provided mechanical insights, yielding stress-strain plots and key parameters such as Young's modulus, ultimate tensile strength, elongation at break, and toughness.

Overall, this comprehensive characterization approach covered material properties, printability,

curing behavior, and mechanical performance, ensuring a thorough understanding of the composite formulations.

2.2.10 3D specimens

Printed and cast samples are realized following ASTM D638, with a type I dumbbell form, for SR349, and ASTM D3039/D3039M, with rectangular form, for PVA.
Samples' names are schematized as XYZ, where X is referred to matrix type (SR for SR349 and PVA); Y represents the filler type (S for silica, C for leather); Z is the filler fraction related to the matrix.

3 Results

3.1 LCA

Environmental impacts were calculated through LCA approach, in which 1 kg of virgin leather, acrylic resin, and recycled leather (waste + raw hides) was compared. Table 1 summarized results.

Table 1: LCA analysis comparison on selected materials.

Parameters	Virgin leather	Acrylic resin	Recycled leather
Climate change [kg CO_2 eq]	11.51	4.35	1.56
Acidification [kg SO_2 eq]	0.42	0.04	0.03

In the following Figure 1 and Figure 2, a comparison in function of recycled leather were done, taken the virgin leather values as 100% of impact.

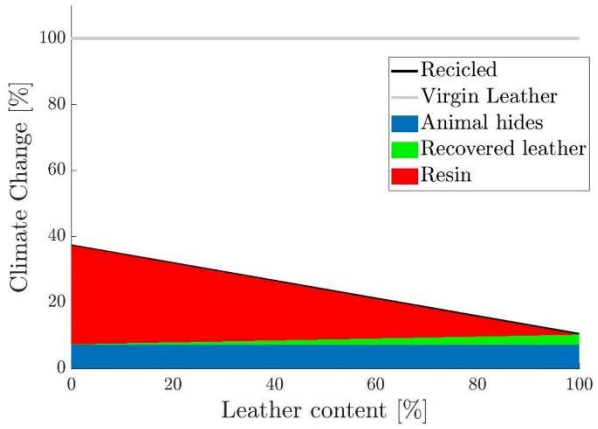

Figure 1: Climate Change comparison between virgin and recycled leather.

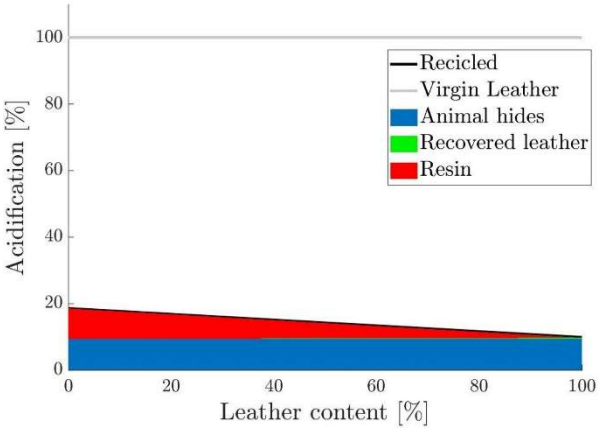

Figure 2: Acidification comparison between virgin and recycled leather.

3.2 Filler dimensional characterization

Optical microscope was used to investigate 50 photos of sieved and non-sieved leather, with 50X lens. Filler parameter P, Eq. 2, described their form. Results are reported in Table 2.

Table 2: Average results of P and diameter filler.

	P	d [mm]
Non-sieved leather	0.312	0.720
Sieved leather	0.375	0.574

3.3 Rheological tests

In every rheological test of SR349 and PVA, opposite behavior is observed between the two fillers used. In silica case, as the concentration increases, the crosspoint between G' and G'' increases, resulting in higher yield stress and strain. The opposite is true for leather. Higher quantities lead to lower crosspoints, higher yield stress, but lower yield strain. All samples containing leather exhibit solid-like behavior immediately after the start of the third step (thixotropy test).

3.4 Printability tests

In printability tests, only formulations with leather are taken into account. All formulations undergo assessment for printability and stability; however, in the case of SR349, the leather swelling during functionalization process, led to intermittent nozzle clogging during printing. This resulted in a disrupted material flow, impeding the ability to

achieve homogeneous printing. So, no result is reported.
As regard PVA, through Eq. 3 and Eq. 4, uniformity and printability index are show in Table 3.

Table 3: Filament uniformity and printability index of PVACX.

Sample	U	Pr
PVAC20	0.12	1.06
PVAC25	0.13	1.13
PVAC30	0.11	1.24

Filament fusion test is shown in Figure 3. All three formulations exhibit excellent printing performance, displaying no noticeable differences. Nevertheless, PVAC25 and PVAC30 stand out as the best options.

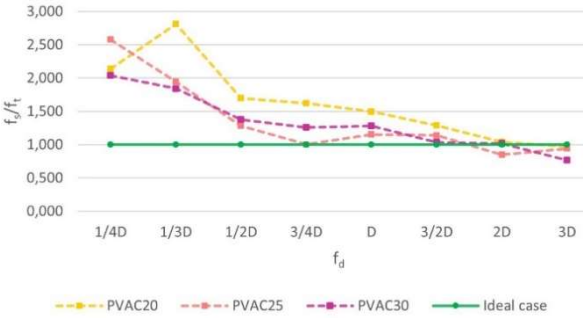

Figure 3: Filament fusion test of PVACX.

3.5 Gel content

Using Eq. 5, gel content percentages of formulations are analyzed. Values are reported in Table 4.

Table 4: Gel content results.

Sample	Gel%
SRC10	92.31
SRC15	91.95
SRC20	83.03
PVAC20	99.19
PVAC25	96.38
PVAC30	89.14

3.6 UV-DSC

It investigates the UV-light curing percentages through the Eq. 6. In both matrixes, UV curing is practically null due to the shielding of UV rays by leather, so results are not reported. This justifies the choice of using a dual curing strategy.

3.7 DSC

The test permits to find the thermal curing percentages, using Eq. 6, and the T_g of materials. Table 5 summarized results.

Table 5: DSC results.

Sample	Curing%	T_g [°C]
SRC10	87.95	43.96
SRC15	81.06	45.03
SRC20	98.48	45.24
PVAC20	72.17	43.83
PVAC25	90.89	47.26
PVAC30	88.74	47.08

3.8 Uniaxial tensile test

In this test mechanical properties are evaluated, as Young's modulus (E), elongation (ε_b) and stress (σ_b) at break, and toughness (k).
In SR case, a comparison between leather and silica cast is made, as observed in Figure 4.

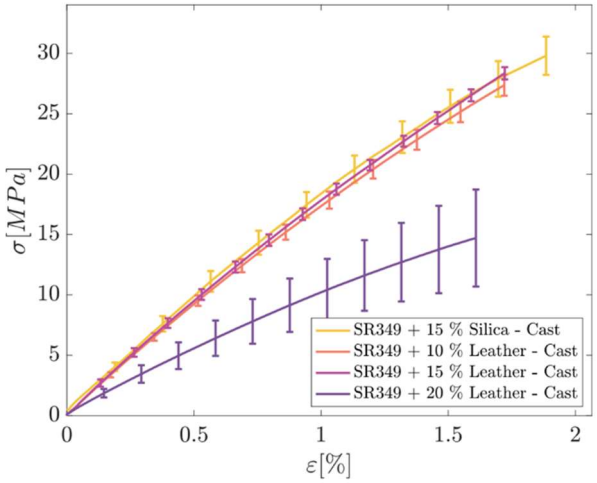

Figure 4: Tensile test of SRCX.

Average values of mechanical properties are reported in Table 6.

Table 6: Average values of SRCX mechanical properties.

Sample	E [GPa]	σ_b [MPa]	ε_b [%]	k [MPa]
SRC10	1.94	25.88	1.57	22.18
SRC15	1.92	29.55	1.82	29.07
SRC20	1.09	14.04	1.55	12.29

To justify the choice of using glycerol in PVA formulations to enhance the ductility of the material, a first comparison between PVAS with

and without glycerol was made. Figure 5 shows the materials behaviour.

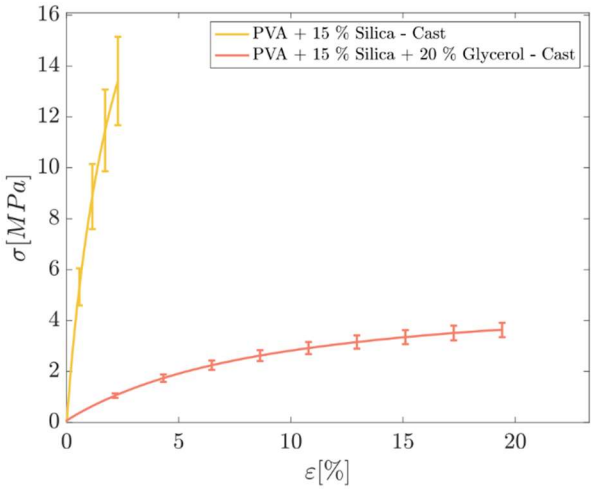

Figure 5: Tensile test of PVAS15 with and without glycerol.

Then, printed and cast PVA with leather and glycerol were tested, and a comparison with PVAS15 was done. Figure 6 illustrates the average curve trends.

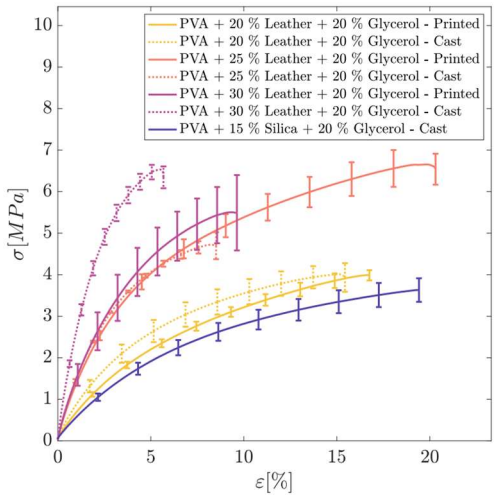

Figure 6: Tensile test of PVACX.

Main properties are reported in Table 7.

Table 7: Average values of PVACX mechanical properties.

Sample	E [MPa]	σ_b [MPa]	ε_b [%]	k [MPa]
PVAC20	74.18	3.96	17.64	47.96
PVAC20 Cast	108.32	4.02	14.63	41.38
PVAC25	170.77	6.67	19.25	94.37
PVAC25 Cast	175.36	4.78	9.17	27.54
PVAC30	178.57	5.72	12.45	50.05
PVAC30 Cast	310.03	6.29	5.95	26.75

A noticeable pattern emerges due to varying leather concentrations. Higher quantities correspond to increased mechanical properties in the specimens, highlighting the reinforcing capability of the leather. In the case of SR, a distinct threshold in filler content becomes evident. Beyond this threshold, mechanical properties experience a significant decline.

4 Conclusions

The addition of leather as reinforcing filler was extremely effective for PVA matrix, while on SR349 was less evident. DSC values confirm the dual curing strategy: thermal curing compensates for the lack of UV cross-linking due to leather screening. As regard printability tests, they were satisfied by PVA formulations, instead SR349 matrix is more suitable for cast. Mechanical properties were enhanced, with the higher leather content. A threshold concentration value is present (very clear in SR349 tests). Consequently, the main goal of this work to demonstrate the potentialities of leather in 3D printing was achieved. Therefore, this strategy is promising also from LCA point of view, reducing the leather industry impact. Some future developments have to be investigated, mainly in printing problem of SR349.

5 References

[1] "Leather Goods Market Size & Growth | Global Report [2030]." https://www.fortunebusinessinsights.com/leather-goods-market-104405 (accessed Nov. 14, 2023).

[2] J. Hu, Z. Xiao, R. Zhou, W. Deng, M. Wang, and S. Ma, "Ecological utilization of leather tannery waste with circular economy model," *J. Clean. Prod.*, vol. 19, no. 2, pp. 221–228, 2011, doi: https://doi.org/10.1016/j.jclepro.2010.09.018.

[3] W. Gao *et al.*, "The status, challenges, and future of additive manufacturing in engineering," *CAD Comput. Aided Des.*, vol. 69, pp. 65–89, 2015, doi: 10.1016/j.cad.2015.04.001.

[4] J. R. Centre and I. for E. and Sustainability, *General guide for Life Cycle Assessment – Provisions and action steps*. Publications Office, 2010.

[5] M. Shou and T. Domenech, "Integrating LCA and blockchain technology to promote circular fashion – A case study of leather handbags," *J. Clean. Prod.*, vol. 373, p. 133557, 2022, doi: https://doi.org/10.1016/j.jclepro.2022.133557.

[6] R. Rajan, E. Rainosalo, M. Lebedevaite, J. Ostrauskaite, and V. Talacka, "Life Cycle Assessment, Optical 3D printing of dental models using acrylic resin based on soybean oils," 2022.